Vascular Tissue Reaction to Acute Malapposition in Human Coronary Arteries

Sequential Assessment With Optical Coherence Tomography

Juan Luis Gutiérrez-Chico, MD, PhD; Joanna Wykrzykowska, MD, PhD; Eveline Nüesch, PhD; Robert Jan van Geuns, MD, PhD; Karel T. Koch, MD, PhD; Jacques J. Koolen, MD, PhD; Carlo di Mario, MD, PhD; Stephan Windecker, MD, PhD; Gerrit-Anne van Es, MSc, PhD; Pierre Gobbens, MSc; Peter Jüni, MD; Evelyn Regar, MD, PhD; Patrick W. Serruys, MD, PhD

Background—The vascular tissue reaction to acute incomplete stent apposition (ISA) is not well known. The aim of this study was to characterize the vascular response to acute ISA in vivo and to look for predictors of incomplete healing.

Methods and Results—Optical coherence tomography studies of 66 stents of different designs, implanted in 43 patients enrolled in 3 randomized trials, were analyzed sequentially after implantation and at 6 to 13 months. Seventy-eight segments with acute ISA were identified in 36 of the patients and matched with the follow-up study by use of fiduciary landmarks. The morphological pattern of healing in the ISA segments was categorized as homogeneous, layered, crenellated, bridged, partially bridged, or bare, depending on the persistence of ISA and on the coverage. After 6 months, acute ISA volume decreased significantly, and 71.5% of the ISA segments were completely integrated into the vessel wall. Segments with acute ISA had higher risk of delayed coverage than well-apposed segments (relative risk 2.37, 95% confidence interval 2.01–2.78). Acute ISA size (estimated as ISA volume or maximum ISA distance per strut) was an independent predictor of ISA persistence and of delayed healing at follow-up.

Conclusions—Neointimal healing tends to reduce ISA, with the malapposed stent struts often integrated completely into the vessel wall, resulting in characteristic morphological patterns. Coverage of ISA segments is delayed with respect to well-apposed segments. The larger the acute ISA, the greater the likelihood of persistent malapposition at follow-up and delayed healing.

Clinical Trial Registration—URL: http://www.clinicaltrials.gov. Unique identifier: NCT00617084 and NCT00934752.

(*Circ Cardiovasc Interv*. 2012;5:20-29.)

Key Words: coronary vessels ■ coronary stenosis ■ percutaneous transluminal angioplasty ■ stents ■ drug-eluting stents ■ neointima ■ tomography, optical coherence

The vascular tissue reaction to acute incomplete stent apposition (ISA) is not well known. The neointimal healing process after stenting might spontaneously correct ISA to some extent, integrating the malapposed regions into the vessel wall, as suggested by sequential quantitative studies with optical coherence tomography (OCT), which reported ISA volumes and percentage of ISA struts decreasing over time.[1–4] Other qualitative OCT studies have also speculated about some morphological patterns at follow-up and the hypothesis that they could represent the vascular response to acutely malapposed struts.[5] The reasons why the vascular biology succeeds in covering and even integrating some ISA regions into the vessel wall but not others remain poorly understood.

ISA has been linked to delayed neointimal coverage in 2 different scenarios: late-acquired ISA and acute ISA. Intravascular ultrasound studies reported the association between ISA and late or very late stent thrombosis[6,7] in the relatively rare clinical context of delayed hypersensitivity to drug-eluting stents, probably triggered by the polymer and recruiting preferentially eosinophils.[8,9] Vasculitis of the 3 arterial layers resulted in weakening of the vessel wall, aneurysmatic

Received July 5, 2011; accepted December 22, 2011.

From the Erasmus Medical Centre–Thoraxcentre, Rotterdam, The Netherlands (J.L.G.-C., J.W., E.R., P.W.S., R.J.v.G.); Institute for Social and Preventive Medicine, University of Bern, Bern, Switzerland (E.N., P.J.); CTU Bern, Bern University Hospital, Bern, Switzerland (E.N., P.J.); Academisch Medisch Centrum, Amsterdam, The Netherlands (K.T.K.); Catharina Ziekenhuis, Eindhoven, The Netherlands (J.J.K.); Cardiovascular Biomedical Research Unit, Royal Brompton and Harefield NHS Trust, London, United Kingdom (C.d.M.); Schweizerisches Herzzentrum–Inselspital, Bern, Switzerland (S.W.); and Cardialysis BV, Rotterdam, The Netherlands (G.-A.v.E., P.G.).

The online-only Data Supplement is available with this article at http://circinterventions.ahajournals.org/lookup/suppl/doi:10.1161/CIRCINTERVENTIONS.111.965301/-/DC1.

Correspondence to Professor Patrick W. Serruys, MD, PhD, Head of Interventional Cardiology, Erasmus MC, Thoraxcenter, Ba583a., 's-Gravendijkwal 230, 3015 CE Rotterdam, The Netherlands. E-mail p.w.j.c.serruys@erasmusmc.nl or jlgutierrez@medynet.com

dilatation, late-acquired ISA, and thrombosis.[6,8,9] In this context, late-acquired ISA struts presented signs of delayed neointimal coverage.[9] On the other hand, the association between acute ISA and delayed coverage has been demonstrated only recently.[1,10] This association provided some supporting evidence for the optimization of apposition aimed at promoting better coverage of the stent. Nevertheless, regions of minimal acute ISA size appear frequently covered and even totally integrated in the vessel wall at follow-up.[2,3] Thus, the question of what degree of acute ISA is worth correcting remains unanswered for the interventional cardiologist.

The aims of the present study were to describe the vascular tissue reaction to acute ISA in human coronary arteries after 6 months, to characterize quantitatively different morphological patterns in terms of apposition and coverage, and to look for predictors at baseline of persisting ISA and delayed coverage.

WHAT IS KNOWN

- Late malapposition has been linked to delayed coverage of stent struts and to stent thrombosis.
- Late malapposition can be the consequence of an inflammatory process (late-acquired malapposition) or of acute malapposition (persisting malapposition).

WHAT THE STUDY ADDS

- The neointimal healing process tends to reduce stent malapposition over time, which results in complete integration of the malapposed struts into the vessel wall in 71.5% of the cases.
- Coverage of acutely malapposed segments is delayed with respect to well-apposed segments in a sequential and matched cohort (relative risk 2.37, 95% confidence interval 2.01–2.78).
- The larger the acute malapposition, the greater the likelihood of persistent malapposed segments at follow-up and delayed healing.

Methods

Study Sample

OCT images from 3 different randomized trials were analyzed: the RESOLUTE-All Comers trial (Randomized, Two-Arm, Noninferiority Study Comparing Endeavor-Resolute Stent With Abbott Xience-V Stent; NCT00617084),[11,12] the De Novo Pilot Study (NCT00934752),[3] and the SECRITT trial (Shield Evaluated at Cardiac Hospital in Rotterdam for Investigation and Treatment of TCFA).[13]

The RESOLUTE-All Comers trial compared a zotarolimus-eluting stent with a hydrophilic-polymer coating (Resolute; Medtronic Cardio Vascular, Santa Rosa, CA) versus an everolimus-eluting stent with fluoropolymer (Xience V; Abbott Vascular, Santa Clara, CA) in a nonselected all-comers population.[11] Twenty percent of the enrolled patients were randomly allocated to angiographic follow-up at 13 months. The patients undergoing angiographic follow-up in selected OCT centers were included in an OCT substudy, with the proportion of covered struts at 13 months as the primary end point.[12] A sequential OCT study was not mandatory per protocol.

The De Novo Pilot Study assessed the performance of a paclitaxel-coated balloon (Moxy; Lutonix Inc, Maple Grove, MN) in combination with a bare-metal stent (Multi-link Vision/MiniVision; Abbott Vascular, Santa Clara, CA) for the treatment of de novo coronary lesions. Myocardial infarction was an exclusion criterion for this study, and a single lesion per patient could be included. The trial randomized the sequence of application (balloon first versus stent first), with a primary end point of percent neointimal volume obstruction assessed by OCT at 6 months.[3]

The SECRITT trial studied the efficacy of a nitinol self-expandable bare-metal stent with ultrathin struts (56 μm) and low chronic outward force (vProtect Luminal Shield; Prescient Medical Inc, Doylestown, PA) for the treatment of high-risk thin-cap fibroatheromas.[13] Patients undergoing catheterization for stable or unstable angina were included if the culprit lesion met the following criteria: (1) Intermediate 40% to 50% diameter stenosis on quantitative coronary angiography; (2) fractional flow reserve $>$0.75; and (3) morphology of thin-cap fibroatheromas in the combination of intravascular ultrasound radiofrequency and OCT studies, as described previously.[14,15] Patients were randomized to receive a self-expandable bare-metal stent or medical therapy. OCT follow-up was scheduled after 6 months.

In the 3 trials, the optimization of PCI results was guided by angiography; therefore, no additional intervention was performed after stent implantation and OCT acquisition, irrespective of the findings in the OCT images.

OCT Study and Analysis

OCT pullbacks were obtained with M2, M3, or C7 systems (Lightlab Imaging; Westford, MA), according to availability at the participating sites, by use of occlusive or nonocclusive techniques as appropriate.[16] Online-only Data Supplement Table 1 summarizes the patients studied with each system and the corresponding technical specifications. Infusion of intracoronary nitroglycerin before OCT pullback was strongly encouraged.

OCT pullbacks were analyzed offline in a core laboratory (Cardialysis BV, Rotterdam, The Netherlands) by independent staff blinded to stent-type allocation and clinical and procedural characteristics of the patients, using proprietary software (Lightlab Imaging). Cross sections were analyzed at 1-mm longitudinal intervals within the stented segment. A metallic strut typically appears as a bright signal-intense structure with dorsal shadowing. Apposition was assessed strut by strut by measuring the distance between the strut marker and the lumen contour. The marker of each strut was placed at the adluminal leading edge, in the midpoint of its long axis, and the distance was measured following a straight line that connected this marker with the center of gravity of the vessel.[17] Struts were classified as ISA if the distance between the strut marker and the lumen contour was greater than the specific strut (plus polymer) thickness.[12,18] This resulted in ISA thresholds of $>$89 μm for everolimus-eluting stents, $>$97 μm for zotarolimus-eluting stents, $>$81 μm for a drug-coated balloon in combination with a bare-metal stent, and $>$56 μm for self-expandable bare-metal stents. Struts located at the ostium of side branches, with no vessel wall behind them, were labeled as nonapposed side-branch struts and excluded from the analysis of apposition.[3,4,10,12] Struts were classified as uncovered if any part of the strut was visibly exposed to the lumen or as covered if a layer of tissue was visible over all the reflecting surfaces.[3,4,10,12,19–24]

ISA Segments, Matching, and Morphological Patterns at Follow-Up

ISA segments were defined as $\geq$2 consecutive cross sections that contained ISA struts immediately after implantation (baseline). ISA segments extended proximally and distally to fiduciary landmarks in the vicinity of the most proximal and distal ISA cross sections. These fiduciary landmarks enabled the matching of the ISA segments with the follow-up studies. The vascular reaction to acute malapposition was categorized according to the morphological pattern at follow-up as follows: (1) Homogeneous (ISA integrated into the vessel wall,

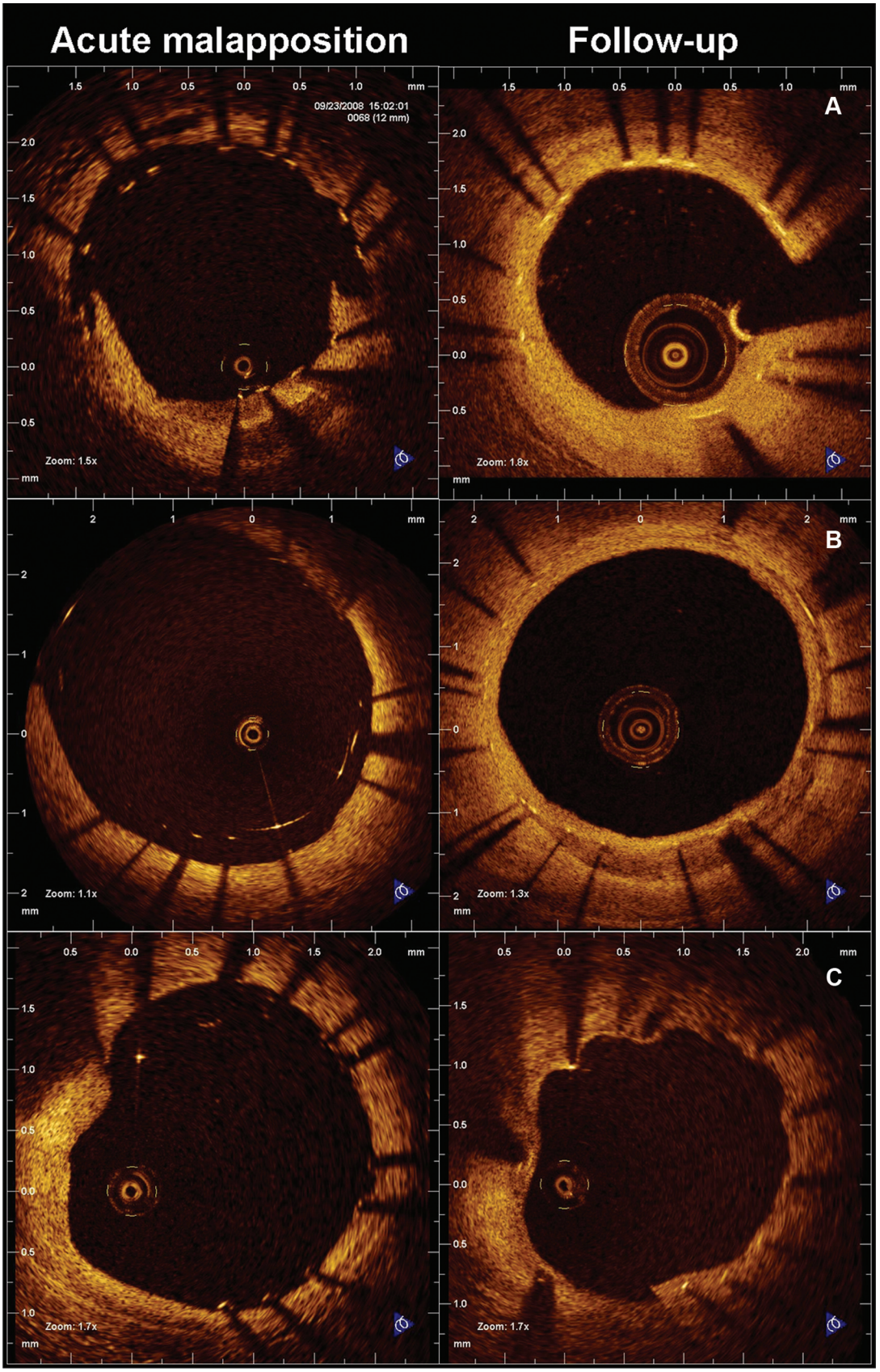

Figure 1. A–C, Vascular reaction to acute malapposition, categorized according to morphological pattern at follow-up: Homogeneous (**A**), layered (**B**), or crenellated (**C**). In these patterns, the regions of acute malapposition have been integrated into the arterial wall. **D–F**, Vascular reaction to acute malapposition, categorized according to the morphological pattern at follow-up: Bridged (**D**), partially bridged (**E**), or bare (**F**). In these patterns, the regions of acute malapposition remain malapposed at follow-up.

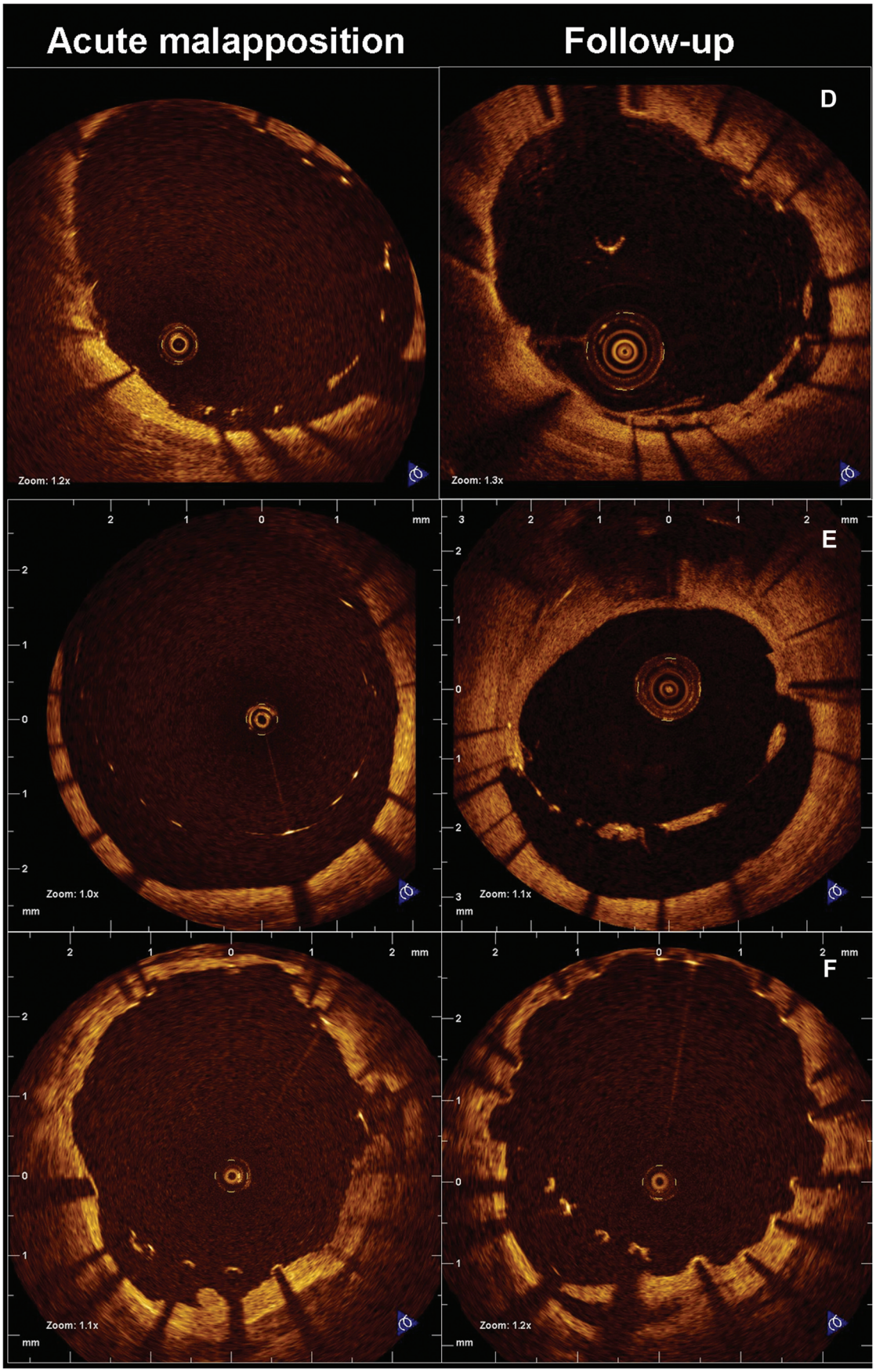

Figure 1 (Continued).

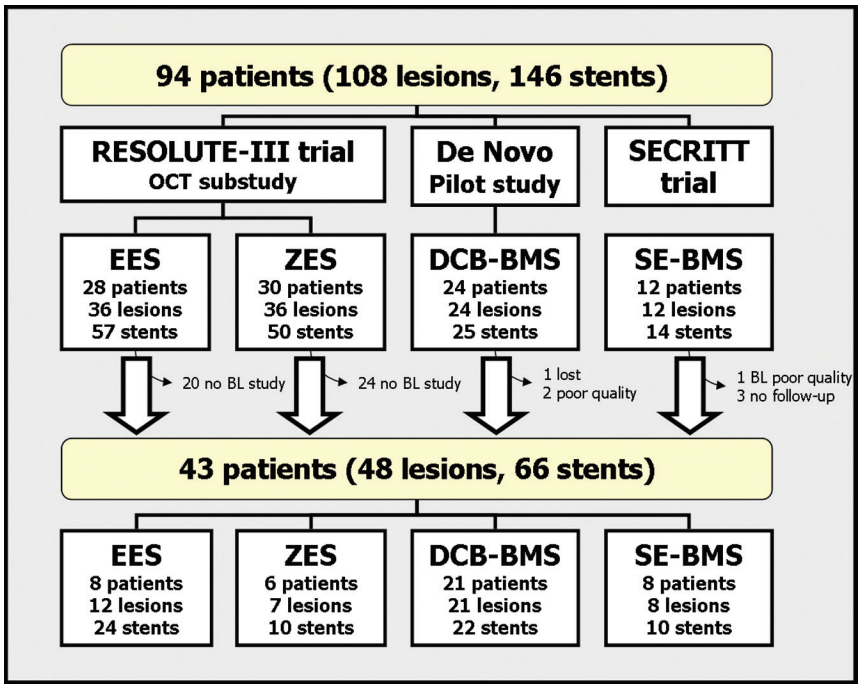

Figure 2. Flow chart summarizing the patients and stents included in the present study, pooled from 3 different randomized trials with optical coherence tomography (OCT). BL indicates baseline study after stent implantation; DCB-BMS, drug-coated balloon in combination with bare-metal stent; EES, everolimus-eluting stent; SE-BMS, self-expandable bare-metal stent; and ZES, zotarolimus-eluting stent.

covered with a homogeneous density, and retaining a smooth lumen contour; Figure 1A); (2) layered (ISA integrated into the vessel wall, covered with a double or triple density, often with a layered appearance, and retaining a smooth lumen contour; Figure 1B); (3) crenellated (ISA integrated into the vessel wall and grossly covered but presenting indentations that gave the lumen contour a scalloped appearance; Figure 1C); (4) bridged (persisting ISA, entirely covered by a rim of tissue linking the vessel intima with the malapposed struts; Figure 1D); (5) partially bridged (persisting ISA; a rim of tissue linking the vessel intima with the malapposed struts could be seen but did not cover all the ISA struts; Figure 1E); or (6) bare (ISA uncovered struts, with scarce tissue reaction, showing a morphological pattern very similar to that observed at baseline; Figure 1F). Delayed healing was defined by patterns 3 through 6; persistent ISA was defined by patterns 4 through 6; grossly delayed healing was defined by patterns 5 and 6. Two independent operators qualitatively classified the ISA segments at follow-up as the worst morphological pattern present in the segment. In case of disagreement, the final category was obtained on consensus after joint review.

Statistical Analysis

Interobserver agreement regarding the classification of the patterns was measured with a quadratic weighted κ-statistic. Continuous variables in the volumetric analysis were compared with multilevel linear regression for paired measurements (baseline versus follow-up) using linear mixed models with the time sequence as the fixed effect and the hierarchical modeling of the measurements as the random effect. Differences in apposition and coverage between the different morphological patterns were analyzed with a Kruskal-Wallis test, and a linear trend among the ranked categories was explored with the Jonckheere-Terpstra test. The relative risk for delayed coverage of ISA versus well-apposed segments was calculated by pooled analysis with an inverse-variance random effects model, taking into account the between-clusters and within-cluster variability and considering each stent as an independent unit of clustering.[10] Predictors of persistent ISA, grossly delayed coverage, percent of ISA, and percent of uncovered struts were studied by multilevel regression using generalized estimating equations to correct for clustering of data. The goodness of fit of the model that contained the significant predictors of the effect was estimated by the corrected quasi-likelihood under the independence model criterion (QICC); the lower the QICC values, the better the fit of the model. Calculations were performed with PASW 17.0 (Chicago, IL) and CMA version 2 (Biostat Inc, Englewood, NJ) software packages.

Results

Forty-eight lesions and 66 stents implanted in 43 patients were ultimately available for sequential analysis among the population included in the present study (Figure 2). Tables 1 and 2 summarize the baseline clinical and procedural characteristics of the patients and angiographic characteristics of the lesions, respectively. Seventy-eight segments with acute ISA were identified in 36 patients at baseline. Matching with the OCT at follow-up was not possible in 8 segments because of lack of fiduciary landmarks (3 cases), out-of-image artifact (3 cases), or incomplete follow-up pullbacks that did not include the ISA segment (2 cases). The following results correspond to the 70 matched segments (32 patients).

Analysis of Morphological Patterns at Follow-Up

The distribution of the morphological patterns at follow-up in the ISA segments is provided in online-only Data Supplement Table 2. The agreement between the initial classifications of the 2 observers was very high (weighted κ 0.96, 95% confidence interval 0.94–0.98). The most frequent pattern was the homogeneous pattern (32.9%), with decreasing proportions in the subsequent ordered patterns, up to the bare pattern (2.9%). Of the analyzed segments, 71.5% had a pattern of spontaneous reapposition onto the vessel wall. The proportion of uncovered, ISA, and ISA-uncovered struts in the quantitative analysis varied significantly between the patterns ($P<0.0001$), following a significant linear trend in the ranked categories ($P<0.0001$; Table 3; Figure 3). The most significant step-up for delayed coverage was observed between the layered and crenellated categories (median percentage of uncovered struts 0.0% and 10.0%, respectively), whereas the most significant step-up for ISA was observed

Table 1. Patient and Procedural Baseline Characteristics

	Patients (n=43)
Age, y	60.4 (10.8)
Males, n (%)	35 (81.4)
Cardiovascular risk factors, n (%)	
Hypertension	23 (53.5)
Diabetes mellitus	8 (18.6)
Insulin-requiring	1 (2.3)
Hypercholesterolemia	33 (76.7)
Smoking	20 (46.5)
Current smoker (<30 d)	10 (23.3)
Family history of CHD	17 (39.5)
Antecedents, n (%)	
Previous MI	15 (34.9)
Previous PCI	9 (20.9)
Previous CABG	2 (4.7)
Clinical presentation, n (%)	
TCFA	8 (18.6)
Silent ischemia	1 (2.3)
Stable angina	19 (44.2)
Unstable angina	12 (27.9)
Myocardial infarction	3 (7.0)
STEMI	2 (4.7)
Procedural characteristics	
No. of vessels treated	1.43 (0.63)
No. of lesions treated	1.62 (0.79)
No. of stents implanted	1.67 (1.27)
Total stented length, mm	30.4 (29.9)
Small vessel (<2.5 mm diameter), n (%)	20 (46.5)
Overlap, n (%)	7 (16.3)
Type of stent, n (%)	
EES	8 (18.6)
ZES	6 (14.0)
DCB-BMS	21 (48.8)
SE-BMS	8 (18.6)

CHD indicates coronary heart disease; MI, myocardial infarction; PCI, percutaneous coronary intervention; CABG, coronary artery bypass graft; TCFA, thin cap fibroatheroma; STEMI, ST-elevation myocardial infarction; EES, everolimus-eluting stent; ZES, zotarolimus-eluting stent; DCB-BMS, combination of drug-coated balloon with bare-metal stent; SE-BMS, self-expandable bare-metal stent.

between crenellated and bridged (median percentage of ISA struts 0.0% and 13.7%, respectively).

Quantitative Analysis of ISA Segments

Three segments were excluded from the quantitative analysis because ISA was located at one of the stent edges, with very different vessel-catheter coaxiality between baseline and follow-up studies, thus making the sequential volumetric calculations unreliable. Table 4 shows the volumetric analysis of the ISA segments. A significant reduction in lumen and ISA areas was observed (online-only Data Supplement Figure 1).

Table 2. Angiographic Characteristics of the Lesions

	Lesions (n=48)
Target vessel, n (%)	
LAD	19 (39.6)
LCx	5 (10.4)
RCA	23 (47.9)
Total occlusion, n (%)	3 (6.3)
Ostial lesion, n (%)	1 (2.1)
Bifurcation, n (%)	12 (25.0)
Moderate or severe calcification, n (%)	9 (18.8)
QCA characteristics, mean (SD)	
Lesion length, mm	12.7 (7.7)
Before stenting	
RVD, mm	2.62 (0.46)
MLD, mm	1.04 (0.60)
Percent diameter stenosis	61.03 (20.35)
Poststenting in-stent	
RVD, mm	2.74 (0.39)
MLD, mm	2.29 (0.42)
Percent diameter stenosis	13.97 (8.11)

LAD indicates left anterior descending coronary artery; LCx, left circumflex coronary artery; RCA, right coronary artery; QCA, quantitative coronary angiography; RVD, reference vessel diameter; MLD, minimal lumen diameter.

Raw per-strut analysis of apposition and coverage is provided in online-only Data Supplement Table 3. The raw proportion of ISA struts in ISA segments was reduced from 37.7% at baseline to 11.8% at follow-up. The incidence of delayed coverage in the ISA segments was 15.4% versus 5.9% in the corresponding well-apposed segments of the same stents (pooled relative risk 2.37; 95% confidence interval 2.01–2.78; online-only Data Supplement Table 4 and online-only Data Supplement Figure 2).

Predictors of Persistence of ISA and of Delayed Coverage

Type of stent and 1 estimator of the ISA size at baseline (either ISA volume or maximum distance to the vessel wall per strut) were tested as predictors of the vascular healing

Table 3. Percentage of Uncovered, ISA, and ISA-Uncovered Struts in Segments With Acute Malapposition, According to Morphological Pattern at Follow-Up

	% of Struts		
Pattern	Uncovered	ISA	ISA-Uncovered
Homogeneous	0.0 (0.0–0.0)	0.0 (0.0–0.0)	0.0 (0.0–0.0)
Layered	0.0 (0.0–0.0)	0.0 (0.0–0.0)	0.0 (0.0–0.0)
Crenellated	10.0 (0.0–24.0)	0.0 (0.0–7.8)	0.0 (0.0–4.2)
Bridged	8.2 (6.0–23.5)	13.7 (0.0–18.8)	1.3 (0.0–8.3)
Partially bridged	21.0 (9.8–32.0)	17.4 (13.5–24.1)	10.3 (5.5–15.9)
Bare	17.1 (12.5–21.7)	10.7 (8.3–13.0)	7.5 (6.3–8.7)

Values are median (25th percentile–75th percentile); n=70 segments, 32 patients.

ISA indicates incomplete stent apposition.

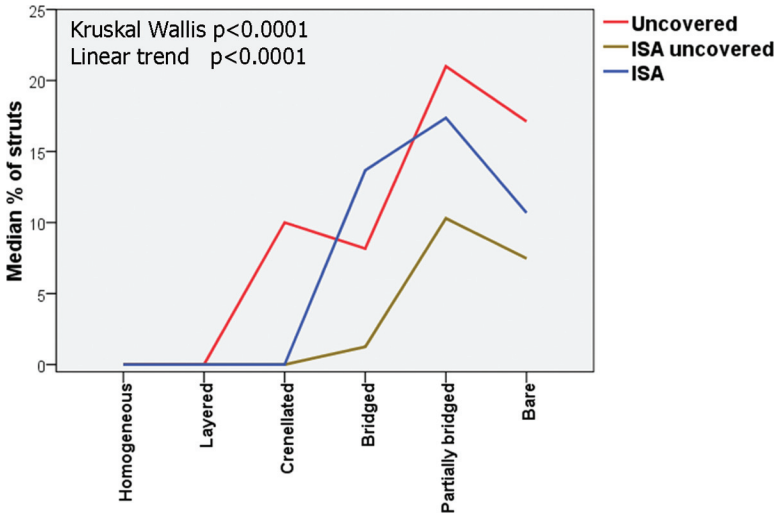

Figure 3. Graphic showing the median percentage of uncovered, ISA, and ISA-uncovered struts in the segments with acute malapposition according to the morphological pattern at follow-up. ISA indicates incomplete stent apposition.

reaction at follow-up. ISA size was the only independent predictor of a pattern of persistent ISA or grossly delayed coverage at follow-up, with similar predictive value when ISA size was estimated by ISA volume as when it was estimated by the maximum ISA distance per strut (online-only Data Supplement Figure 3). ISA size and the type of stent were both independent predictors of a pattern of delayed coverage, with similar predictive values for the models with ISA volume or with maximum ISA distance per strut as estimators of ISA size. The percentage of ISA struts in the segment at follow-up could be predicted by the ISA volume after implantation ($P \leq 0.0001$; QICC 336.87) or by the maximum ISA distance per strut ($P \leq 0.0001$; QICC 342.64) alone, whereas the percentage of uncovered struts at follow-up was predicted by ISA size after implantation ($P=0.02$ for ISA volume, $P=0.04$ for maximum ISA distance per strut) and by the type of stent ($P=0.045$; QICC 5056.30 for the model with ISA volume and QICC 5389.10 for the model with maximum ISA distance per strut).

Table 5 shows an estimation of the likelihood at follow-up of resolved versus persistent ISA and of grossly covered versus grossly delayed patterns of healing, based on the analysis of the present sample. Maximum ISA distances <270 μm after stent implantation appeared grossly covered and spontaneously reapposed in 100% of cases at follow-up, whereas maximum ISA distances ≥ 850 μm resulted in persisting ISA and grossly delayed coverage in 100% of cases.

Clinical Outcomes

At the time of OCT follow-up, 6 patients had experienced major adverse cardiovascular events, all of them in the group with a drug-coated balloon in combination with a bare-metal stent: 1 periprocedural non–Q-wave MI, 1 target-vessel–related non–Q-wave MI at follow-up, and 4 clinically driven target-vessel revascularizations (because of stable angina). No case of stent thrombosis occurred in any of the subgroups.

Discussion

The main findings of the present study are as follows: (1) The vascular tissue reaction to acute ISA can be described by OCT according to simple morphological patterns that represent different degrees of persisting malapposition and coverage. (2) The neointimal response tends to reduce ISA size, often resulting in the malapposed struts being completely integrated into the vessel wall. (3) Within the same stent, coverage of ISA segments is delayed with respect to that of well-apposed segments. (4) The size of acute ISA is directly associated with its persistence at follow-up and with delayed coverage.

To the best of our knowledge, this is the first sequential OCT study describing the healing process of acute ISA both

Table 4. Areas and Volumetric Analysis of ISA Segments, Baseline Versus Follow-Up Results

				95% CI		
	Baseline	Follow-Up	Mean Difference	Lower	Upper	*P*
Length, mm	2.0 (0.3)	1.9 (0.3)	−0.1 (0.5)	−1.1	0.8	0.780
MLA, mm^2	8.05 (0.32)	6.71 (0.32)	−1.34 (0.45)	−2.23	−0.45	0.003
Mean lumen area, mm^2	8.47 (0.33)	7.14 (0.33)	−1.33 (0.47)	−2.25	−0.42	0.005
Mean stent area, mm^2	8.09 (0.31)	7.99 (0.31)	−0.10 (0.44)	−0.97	0.77	0.819
Maximum ISA area, mm^2	0.79 (0.11)	0.29 (0.11)	−0.50 (0.16)	−0.82	−0.19	0.002
Mean ISA area, mm^2	0.60 (0.08)	0.19 (0.08)	−0.41 (0.11)	−0.62	−0.20	<0.0001
ISA volume, mm^3	1.44 (0.40)	0.68 (0.40)	−0.76 (0.57)	−1.89	0.37	0.184

Values are mean (SE). n=67 segments 30 patients.
ISA indicates incomplete stent apposition; CI, confidence interval; MLA, minimal lumen area.

Table 5. Predictive Values for Resolved vs Persistent ISA and for Grossly Covered Versus Grossly Delayed Healing Patterns at Follow-Up of Different Thresholds of ISA Size at Baseline

	Percentage Likelihood at Follow-Up			
ISA Size at Baseline	Resolved ISA	Grossly Covered	Persistent ISA	Grossly Delayed Healing
ISA volume, mm^3				
<0.1	100	100	. . .	. . .
<0.2	96.9	100	. . .	. . .
<2.5	84.5	93.4	. . .	. . .
<4.4	79.0	93.1	. . .	. . .
<12.5	74.2	89.4	. . .	. . .
≥0.1	. . .	. . .	34.6	18.6
≥0.2	. . .	. . .	47.2	22.9
≥2.5	. . .	. . .	100	44.4
≥4.4	. . .	. . .	100	66.7
≥12.5	. . .	. . .	100	100
Maximum ISA distance, μm				
<270	100	100	. . .	. . .
<350	94.9	100	. . .	. . .
<400	92.7	97.6	. . .	. . .
<520	83.3	92.6	. . .	. . .
<850	75.4	87.9	. . .	. . .
≥270	. . .	. . .	46.15	20.5
≥350	. . .	. . .	57.1	26.9
≥400	. . .	. . .	57.7	28.6
≥520	. . .	. . .	69.2	30.8
≥850	. . .	. . .	100	100

n=67 Segments, 30 patients.
ISA indicates incomplete stent apposition.

qualitatively and quantitatively and the first to link simple morphological qualitative patterns of healing with specific malapposition and coverage rates in the subsequent quantitative analysis. This observation might enable semiquantitative estimations of coverage and apposition, which could be potentially useful for in situ clinical decision making.

The vascular tissue reaction ends in the complete integration of the ISA into the vessel wall in most cases (71.5%), but 2 of 3 cases of acute ISA have a morphological healing pattern other than homogeneous. This might represent the in vivo correlate of some experimental observations: (1) Reendothelialization that ensues after a vessel injury occurs by proliferation of endothelial and smooth muscle cells, starting from the uninjured margins until the endothelial continuity is restored.[25–29] At this point, the confluence of endothelial cells inhibits their own proliferation and stimulates the secretion of heparin sulfates, which in turn inhibit the proliferation of smooth muscle cells.[30] According to this confluent model, endothelial cells would spread out on the surface of the malapposed struts, resulting in conformal coverage of the detached mesh. The bridged pattern might represent the maturation of this neointimal conformal coverage. (2) This reendothelialization process is limited in time[26–28]: It stops after 2 weeks (in the rabbit) or after 6 weeks (in the rat), regardless of whether endothelial continuity has been restored.[25,29] The partially bridged and bare patterns (grouped as "grossly delayed coverage") might represent the failure of neointima to cover large ISA regions before the vascular healing response ceases. This is consistent with our finding of large acute ISA volumes associated with patterns of grossly delayed coverage at follow-up. Likewise, small ISA volumes could induce a conformal bridged pattern of healing that ends up connecting the ISA struts with the vessel wall (homogeneous pattern) or that creates a false lumen that undergoes subsequent low-flow and thrombosis phenomena (layered pattern). The layered pattern might also be caused by the cytotoxicity of specific drugs or stents[31] or by the increased presence of fibrinoid or proteoglycans.[32,33] Finally, the crenellated pattern has been proposed to be the result of a vascular reaction to acute ISA.[5] The present findings confirm the hypothesis that the crenellated pattern appears as 1 of the possible vascular reactions to acute ISA and is associated with delayed coverage. The abnormally hyporeactive neointima that leads to a bare pattern might reflect something other than the mere failure to restore a too large ISA region and deserves further investigation.

The quantitative results constitute additional and definitive evidence about the higher risk of delayed coverage associated with acute ISA, as suggested and demonstrated by previous OCT studies.[1,10] This is a truly sequential study with the finest level of matching possible (segments), thus complementing the limitations of previous analytic studies.[10] Although the evidence provided by this approach is only at an ecological level (ie, the uncovered struts could theoretically be the well-apposed struts in the segment), the consistency with previous studies that used different approaches[1,10] should constitute definitive evidence of the association between acute ISA and delayed coverage.

The larger the ISA, the more likely it is to persist at follow-up and to present a pattern of grossly delayed coverage. The size of acute ISA can be estimated by different parameters. Estimation by ISA volume is very accurate but cannot be accomplished in a straightforward manner; hence, this parameter is of limited utility for decision making in the catheterization laboratory. Conversely, maximum ISA distance per strut can be measured directly in situ and has a predictive value equivalent to that of ISA volume for the persistence of ISA and for coverage; therefore, it might be preferable as an objective criterion for optimization of acute ISA in the catheterization laboratory. Although the present study can provide some rationale for the optimization of apposition, the clinical benefit of such an approach remains unproven. Interestingly, the coverage rate cannot be predicted by ISA size alone (except in cases of grossly delayed coverage) but also depends on the type of stent.

Study Limitations

OCT coverage correlates with histological neointimal healing and endothelialization after stenting in animal models,[21,34] but its sensitivity and specificity in human atherosclerotic vessels

are unknown. For the 14 patients in the RESOLUTE-All Comers trial, the follow-up period was 13 instead of 6 months because of the sustained kinetics of release of the device and to ensure that OCT studies were performed after the neointimal healing process had achieved its maximum potential. The heterogeneity of devices and follow-up periods compels us to classify our results as preliminary and to replicate this analysis in more specific scenarios and larger samples.

Primary stenting in ST-elevation myocardial infarction predisposes to acute ISA.[35] The present sample included only 2 cases with ST-elevation myocardial infarction. Thus, the role of the clinical indication on the healing of ISA requires clarification in larger samples that include more patients with ST-elevation myocardial infarction.[23,24,35]

Conclusions

The neointimal healing process tends to reduce ISA size, often integrating it completely into the vessel wall, and results in characteristic morphological patterns. The coverage of ISA segments is delayed with respect to well-apposed segments. The larger the acute ISA, the greater the likelihood of both persistent malapposition at follow-up and delayed healing.

Sources of Funding

This study pooled data from 3 different randomized trials sponsored by Medtronic Cardio Vascular (Santa Rosa, CA), Lutonix Inc (Maple Grove, MA), and Prescient Medical Inc (Doylestown, PA). The core laboratory and clinical research organization responsible for the analysis (Cardialysis BV, Rotterdam, The Netherlands) received grants from the corresponding sponsors to run the trials. The cost of the research extraclinical activities pertaining to the study protocols was reimbursed to the participating sites by the sponsors, according to the corresponding health service reimbursement.

Disclosures

Drs Windecker and Di Mario have received speakers' fees from the corresponding sponsors. The remaining authors report no conflicts.

References

1. Ozaki Y, Okumura M, Ismail TF, Naruse H, Hattori K, Kan S, Ishikawa M, Kawai T, Takagi Y, Ishii J, Prati F, Serruys PW. The fate of incomplete stent apposition with drug-eluting stents: an optical coherence tomography-based natural history study. *Eur Heart J*. 2010;31:1470–1476.
2. Kim WH, Lee BK, Lee S, Shim JM, Kim JS, Kim BK, Ko YG, Choi D, Jang Y, Hong MK. Serial changes of minimal stent malapposition not detected by intravascular ultrasound: follow-up optical coherence tomography study. *Clin Res Cardiol*. 2010;99:639–644.
3. Gutiérrez-Chico J, van Geuns RJ, Koch K, Koolen J, Duckers HJ, Regar E, Serruys PW. Paclitaxel-coated balloon in combination with bare metal stent for treatment of de novo coronary lesions: an optical coherence tomography first-in-human randomised trial, balloon-first vs. stent first. *EuroIntervention*. 2011;7:711–722.
4. Gutiérrez-Chico J, Jüni P, García-García HM, Regar E, Nüesch E, Borgia F, van der Giessen WJ, Davies S, van Geuns RJ, Secco GG, Meis S, Windecker S, Serruys PW, di Mario C. Long term tissue coverage of a biodegradable polylactide polymer-coated biolimus-eluting stent: comparative sequential assessment with optical coherence tomography until complete resorption of the polymer. *Am Heart J*. 2011;162:922–931.
5. Radu M, Jørgensen E, Kelbæk H, Helqvist S, Skovgaard L, Saunamäki K. Strut apposition after coronary stent implantation visualised with optical coherence tomography. *EuroIntervention*. 2010;6:86–93.
6. Cook S, Wenaweser P, Togni M, Billinger M, Morger C, Seiler C, Vogel R, Hess O, Meier B, Windecker S. Incomplete stent apposition and very late stent thrombosis after drug-eluting stent implantation. *Circulation*. 2007;115:2426–2434.
7. Hassan AKM, Bergheanu SC, Stijnen T, van der Hoeven BL, Snoep JD, Plevier JWM, Schalij MJ, Wouter Jukema J. Late stent malapposition risk is higher after drug-eluting stent compared with bare-metal stent implantation and associates with late stent thrombosis. *Eur Heart J*. 2010;31:1172–1180.
8. Cook S, Ladich E, Nakazawa G, Eshtehardi P, Neidhart M, Vogel R, Togni M, Wenaweser P, Billinger M, Seiler C, Gay S, Meier B, Pichler WJ, Juni P, Virmani R, Windecker S. Correlation of intravascular ultrasound findings with histopathological analysis of thrombus aspirates in patients with very late drug-eluting stent thrombosis. *Circulation*. 2009;120:391–399.
9. Virmani R, Guagliumi G, Farb A, Musumeci G, Grieco N, Motta T, Mihalcsik L, Tespili M, Valsecchi O, Kolodgie FD. Localized hypersensitivity and late coronary thrombosis secondary to a sirolimus-eluting stent: should we be cautious? *Circulation*. 2004;109:701–705.
10. Gutiérrez-Chico JL, Regar E, Nüesch E, Okamura T, Wykrzykowska J, di Mario C, Windecker S, van Es GA, Gobbens P, Jüni P, Serruys PW. Delayed coverage in malapposed and side-branch struts with respect to well-apposed struts in drug-eluting stents. *Circulation*. 2011;124:612–623.
11. Serruys PW, Silber S, Garg S, van Geuns RJ, Richardt G, Buszman PE, Kelbaek H, van Boven AJ, Hofma SH, Linke A, Klauss V, Wijns W, Macaya C, Garot P, DiMario C, Manoharan G, Kornowski R, Ischinger T, Bartorelli A, Ronden J, Bressers M, Gobbens P, Negoita M, van Leeuwen F, Windecker S. Comparison of zotarolimus-eluting and everolimus-eluting coronary stents. *N Engl J Med*. 2010;363:136–146.
12. Gutierrez-Chico JL, van Geuns RJ, Regar E, van der Giessen WJ, Kelbaek H, Saunamaki K, Escaned J, Gonzalo N, Di MC, Borgia F, Nuesch E, Garcia-Garcia HM, Silber S, Windecker S, Serruys PW. Tissue coverage of a hydrophilic polymer-coated zotarolimus-eluting stent vs. a fluoropolymer-coated everolimus-eluting stent at 13-month follow-up: an optical coherence tomography substudy from the RESOLUTE All Comers trial. *Eur Heart J*. 2011;32:2454–2463.
13. Shin ES, Garcia-Garcia HM, Okamura T, Wykrzykowska JJ, Gonzalo N, Shen ZJ, van Geuns RJ, Regar E, Serruys PW. Comparison of acute vessel wall injury after self-expanding stent and conventional balloon-expandable stent implantation: a study with optical coherence tomography. *J Invasive Cardiol*. 2010;22:435–439.
14. Sawada T, Shite J, Garcia-Garcia HM, Shinke T, Watanabe S, Otake H, Matsumoto D, Tanino Y, Ogasawara D, Kawamori H, Kato H, Miyoshi N, Yokoyama M, Serruys PW, Hirata K. Feasibility of combined use of intravascular ultrasound radiofrequency data analysis and optical coherence tomography for detecting thin-cap fibroatheroma. *Eur Heart J*. 2008;29:1136–1146.
15. Gonzalo N, Garcia-Garcia HM, Regar E, Barlis P, Wentzel J, Onuma Y, Ligthart J, Serruys PW. In vivo assessment of high-risk coronary plaques at bifurcations with combined intravascular ultrasound and optical coherence tomography. *J Am Coll Cardiol Cardiovasc Imaging*. 2009;2:473–482.
16. Gonzalo N, Tearney GJ, Serruys PW, van Soest G, Okamura T, Garcia-Garcia HM, van Geuns RJ, van der Ent M, Ligthart JM, Bouma BE, Regar E. Second-generation optical coherence tomography in clinical practice: high-speed data acquisition is highly reproducible in patients undergoing percutaneous coronary intervention. *Rev Esp Cardiol*. 2010;63:893–903.
17. Gonzalo N, Garcia-Garcia HM, Serruys PW, Commissaris KH, Bezerra H, Gobbens P, Costa M, Regar E. Reproducibility of quantitative optical coherence tomography for stent analysis. *EuroIntervention*. 2009;5:224–232.
18. Tanigawa J, Barlis P, di Mario C. Intravascular optical coherence tomography: optimisation of image acquisition and quantitative assessment of stent strut apposition. *EuroIntervention*. 2007;3:128–136.
19. Barlis P, Regar E, Serruys PW, Dimopoulos K, van der Giessen WJ, van Geuns RJ, Ferrante G, Wandel S, Windecker S, Van Es GA, Eerdmans P, Juni P, di Mario C. An optical coherence tomography study of a biodegradable vs. durable polymer-coated limus-eluting stent: a LEADERS trial sub-study. *Eur Heart J*. 2010;31:165–176.
20. Guagliumi G, Musumeci G, Sirbu V, Bezerra HG, Suzuki N, Fiocca L, Matiashvili A, Lortkipanidze N, Trivisonno A, Valsecchi O, Biondi-Zoccai G, Costa MA. Optical coherence tomography assessment of in vivo vascular response after implantation of overlapping bare-metal and drug-eluting stents. *JACC Cardiovasc Interv*. 2010;3:531–539.
21. Templin C, Meyer M, Muller MF, Djonov V, Hlushchuk R, Dimova I, Flueckiger S, Kronen P, Sidler M, Klein K, Nicholls F, Ghadri JR, Weber K, Paunovic D, Corti R, Hoerstrup SP, Luscher TF, Landmesser U.

Coronary optical frequency domain imaging (OFDI) for in vivo evaluation of stent healing: comparison with light and electron microscopy. *Eur Heart J*. 2010;31:1792–1801.
22. Guagliumi G, Sirbu V, Musumeci G, Bezerra HG, Aprile A, Kyono H, Fiocca L, Matiashvili A, Lortkipanidze N, Vassileva A, Popma JJ, Allocco DJ, Dawkins KD, Valsecchi O, Costa MA. Strut coverage and vessel wall response to a new-generation paclitaxel-eluting stent with an ultrathin biodegradable abluminal polymer: Optical Coherence Tomography Drug-Eluting Stent Investigation (OCTDESI). *Circ Cardiovasc Interv*. 2010;3:367–375.
23. Guagliumi G, Sirbu V, Bezerra H, Biondi-Zoccai G, Fiocca L, Musumeci G, Matiashvili A, Lortkipanidze N, Tahara S, Valsecchi O, Costa M. Strut coverage and vessel wall response to zotarolimus-eluting and bare-metal stents implanted in patients with ST-segment elevation myocardial infarction: the OCTAMI (Optical Coherence Tomography in Acute Myocardial Infarction) Study. *JACC Cardiovasc Interv*. 2010;3:680–687.
24. Guagliumi G, Costa MA, Sirbu V, Musumeci G, Bezerra HG, Suzuki N, Matiashvili A, Lortkipanidze N, Mihalcsik L, Trivisonno A, Valsecchi O, Mintz GS, Dressler O, Parise H, Maehara A, Cristea E, Lansky AJ, Mehran R, Stone GW. Strut coverage and late malapposition with paclitaxel-eluting stents compared with bare metal stents in acute myocardial infarction: optical coherence tomography substudy of the Harmonizing Outcomes With Revascularization and Stents in Acute Myocardial Infarction (HORIZONS-AMI) Trial. *Circulation*. 2011;123:274–281.
25. Reidy MA, Standaert D, Schwartz SM. Inhibition of endothelial cell regrowth: cessation of aortic endothelial cell replication after balloon catheter denudation. *Arteriosclerosis*. 1982;2:216–220.
26. Haudenschild CC, Schwartz SM. Endothelial regeneration, II: restitution of endothelial continuity. *Lab Invest*. 1979;41:407–418.
27. Reidy MA, Schwartz SM. Endothelial regeneration, III: time course of intimal changes after small defined injury to rat aortic endothelium. *Lab Invest*. 1981;44:301–308.
28. Bjorkerud S, Bondjers G. Arterial repair and atherosclerosis after mechanical injury, 5: tissue response after induction of a large superficial transverse injury. *Atherosclerosis*. 1973;18:235–255.
29. Reidy MA, Clowes AW, Schwartz SM. Endothelial regeneration, V: inhibition of endothelial regrowth in arteries of rat and rabbit. *Lab Invest*. 1983;49:569–575.
30. Clowes AW, Karnowsky MJ. Suppression by heparin of smooth muscle cell proliferation in injured arteries. *Nature*. 1977;265:625–626.
31. Tanimoto S, Aoki J, Serruys PW, Regar E. Paclitaxel-eluting stent restenosis shows three-layer appearance by optical coherence tomography. *EuroIntervention*. 2006;1:484.
32. Teramoto T, Ikeno F, Otake H, Lyons JK, van Beusekom HM, Fearon WF, Yeung AC. Intriguing peri-strut low-intensity area detected by optical coherence tomography after coronary stent deployment. *Circ J*. 2010;74:1257–1259.
33. van Beusekom HM, Saia F, Zindler JD, Lemos PA, Swager-Ten Hoor SL, van Leeuwen MA, de Feijter PJ, Serruys PW, van der Giessen WJ. Drug-eluting stents show delayed healing: paclitaxel more pronounced than sirolimus. *Eur Heart J*. 2007;28:974–979.
34. Murata A, Wallace-Bradley D, Tellez A, Alviar C, Aboodi M, Sheehy A, Coleman L, Perkins L, Nakazawa G, Mintz G, Kaluza GL, Virmani R, Granada JF. Accuracy of optical coherence tomography in the evaluation of neointimal coverage after stent implantation. *JACC Cardiovasc Imaging*. 2010;3:76–84.
35. Gonzalo N, Barlis P, Serruys PW, Garcia-Garcia HM, Onuma Y, Ligthart J, Regar E. Incomplete stent apposition and delayed tissue coverage are more frequent in drug-eluting stents implanted during primary percutaneous coronary intervention for ST-segment elevation myocardial infarction than in drug-eluting stents implanted for stable/unstable angina: insights from optical coherence tomography. *JACC Cardiovasc Interv*. 2009;2:445–452.

SUPPLEMENTAL MATERIAL.

Supplemental tables.

Supplemental table 1: Technical specifications of the different OCT systems and number of patients studied with each model at baseline and follow-up.

		M2	M3	C7
Technique		Occlusive	Non-occlusive	Non-occlusive
Domain		Time	Time	Fourier
Catheter		ImageWire	ImageWire	Dragonfly
Rotation speed (frames/s)		15.6	20	100
Pullback speed (mm/s)		2	3	10-20
Post-stent implantation	**EES**	1	7	0
	ZES	0	6	0
	DCB-BMS	0	0	21
	SE-BMS	0	6	2
Total nr of patients		**1**	**19**	**22**
Follow-up	**EES**	0	7	1
	ZES	0	6	0
	DCB-BMS	0	0	21
	SE-BMS	0	3	5
Total nr of patients		**0**	**16**	**27**

All systems and catheters from Lightlab Imaging, Westford, Massachusetts, USA.

Supplemental table 2: Morphologic patterns at follow-up in the regions with acute malapposition at baseline, stratified by type of stent.

	Homogeneous	Layered	Crenellated	Bridged	Partially bridged	Bare
EES (n=14)	9 (64.3%)	0 (0.0%)	0 (0.0%)	4 (28.6%)	0 (0.0%)	1 (7.1%)
ZES (n=13)	5 (38.5%)	0 (0.0%)	4 (30.8%)	2 (15.4%)	2 (15.4%)	0 (0.0%)
DCB-BMS (n=31)	9 (29.0%)	11(35.5%)	5 (16.1%)	4 (12.9%)	1 (3.2%)	1 (3.2%)
SE-BMS (n=12)	0 (0.0%)	3 (25.0%)	4 (33.3%)	1 (8.3%)	4 (33.3%)	0 (0.0%)
Total (n=70)	23 (32.9%)	14 (20.0%)	13 (18.6%)	11 (15.7%)	7 (10.0%)	2 (2.9%)

DCB-BMS: Combination of drug-coated balloon with bare metal stent; EES: Everolimus-eluting stent; SE-BMS: Self-expandable bare metal stent; ZES: Zotarolimus-eluting stent.

Supplemental table 3: Analysis per strut of apposition and coverage in the matched stents.

n=66 stents 43 patients		Malapposed stents				Well-apposed stents	
		ISA segments		Well-apposed segments			
		BL	FU	BL	FU	BL	FU
Apposition	Well-apposed	1345 (62.2%)	2164 (87.9%)	5002 (94.4%)	4870 (98.8%)	5347 (99.3%)	5563 (99.7%)
	ISA	815 (37.7%)	290 (11.8%)	237 (4.5%)	19 (0.4%)	6 (0.1%)	3 (0.1%)
	NASB	3 (0.1%)	7 (0.3%)	55 (1.0%)	39 (0.8%)	30 (0.6%)	11 (0.2%)
Uncovered		2163 (100%)	379 (15.4%)	5924 (100%)	289 (5.9%)	5383 (100%)	251 (5.3%)
ISA-uncovered		815 (37.7 %)	146 (5.9%)	237 (4.5%)	16 (0.3%)	6 (0.1%)	3 (0.1%)
TOTAL		2163	2461	5294	4928	5383	5577

Values are count (%) of struts.
BL: Baseline; DCB-BMS: Drug-coated balloon in combination with bare metal stent; EES: Everolimus-eluting stent; FU: Follow-up; ISA: Incomplete stent apposition; NASB: Non-apposed side-branch strut; SE-BMS: Self-expandable bare metal stent; ZES: Zotarolimus-eluting stent.

Supplemental table 4: Relative risk for delayed coverage in ISA vs. non-ISA segments pooled by stent, and stratified by the type of stent.

	n	Magnitude of effect			Heterogeneity of the effect		
		RR	95% CI		p val	I^2	τ^2
			Lower	Upper			
All	52	2.34	2.01	2.78	<0.0001	50.20	0.38
EES	9	4.10	2.52	6.65	0.005	63.92	1.21
ZES	11	2.57	1.98	3.34	0.110	36.15	0.12
DCB+BMS	26	2.01	1.56	2.60	0.010	43.62	0.44
SE-BMS	6	1.68	0.96	2.95	0.036	58.06	0.86

DCB-BMS: Drug-coated balloon in combination with bare metal stent; EES: Everolimus-eluting stent; RR: Relative risk; SE-BMS: Self-expandable bare metal stent; ZES: Zotarolimus-eluting stent.

Supplemental figures.

Supplemental figure 1.

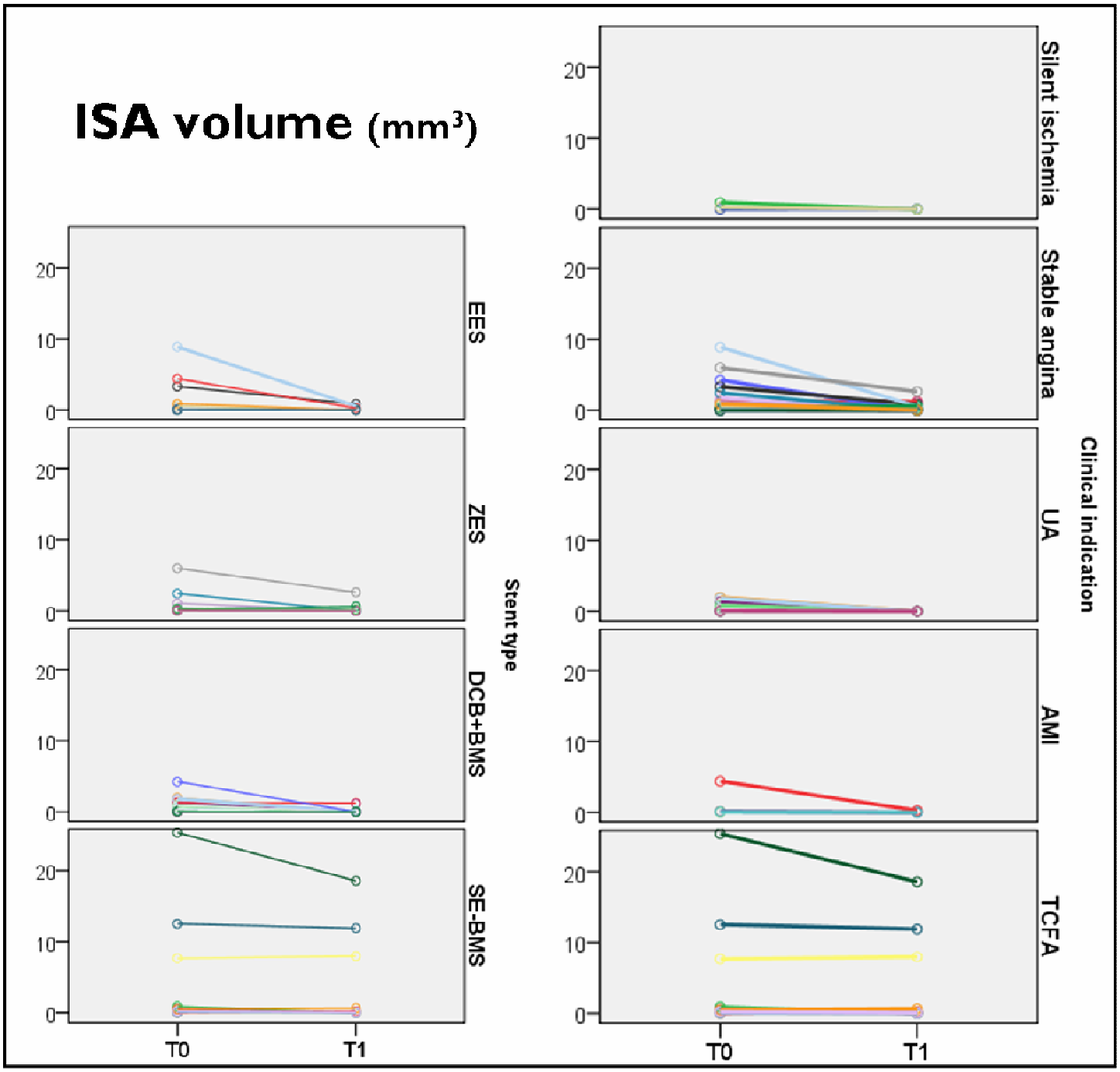

Supplemental figure 2.

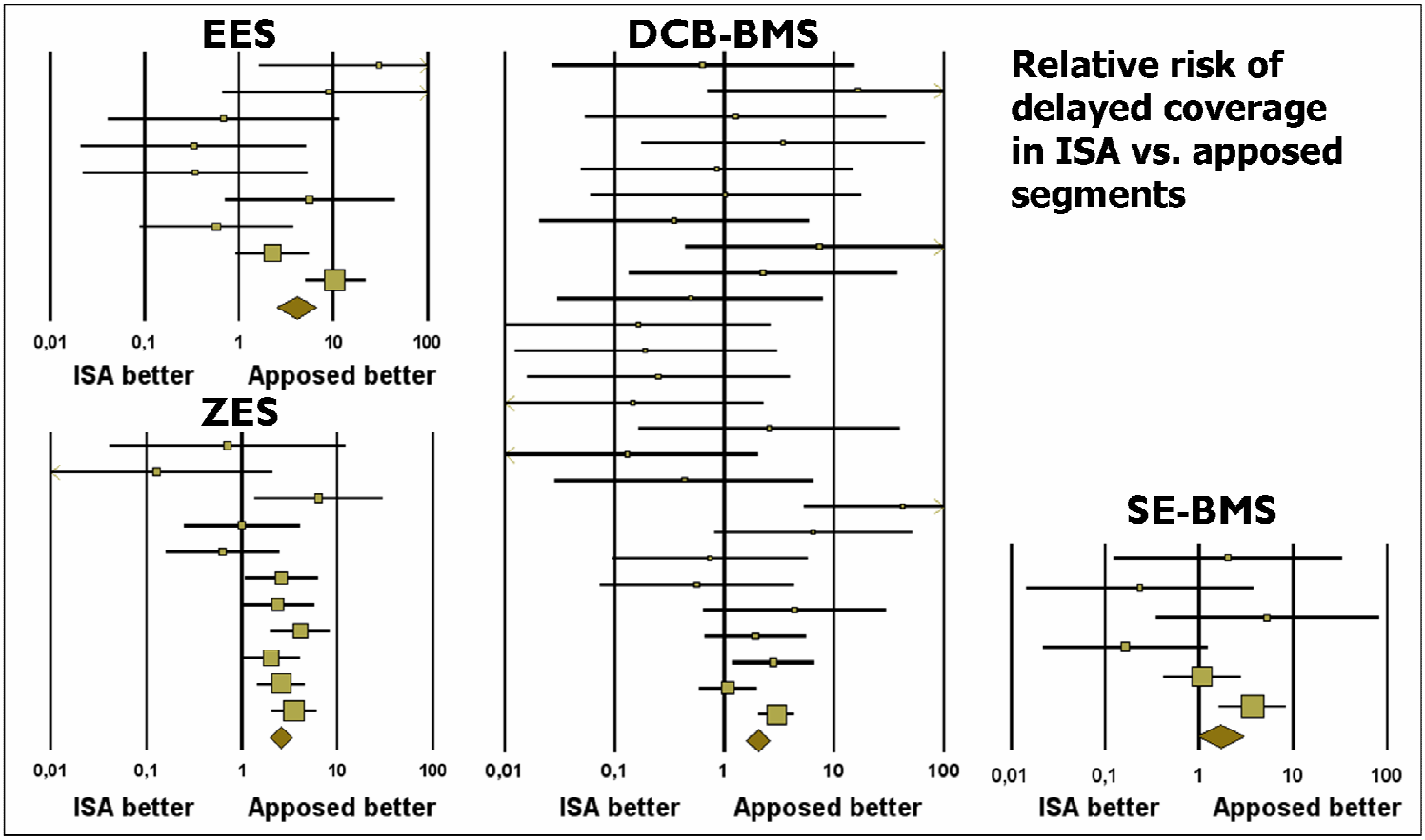

Supplemental figure 3.

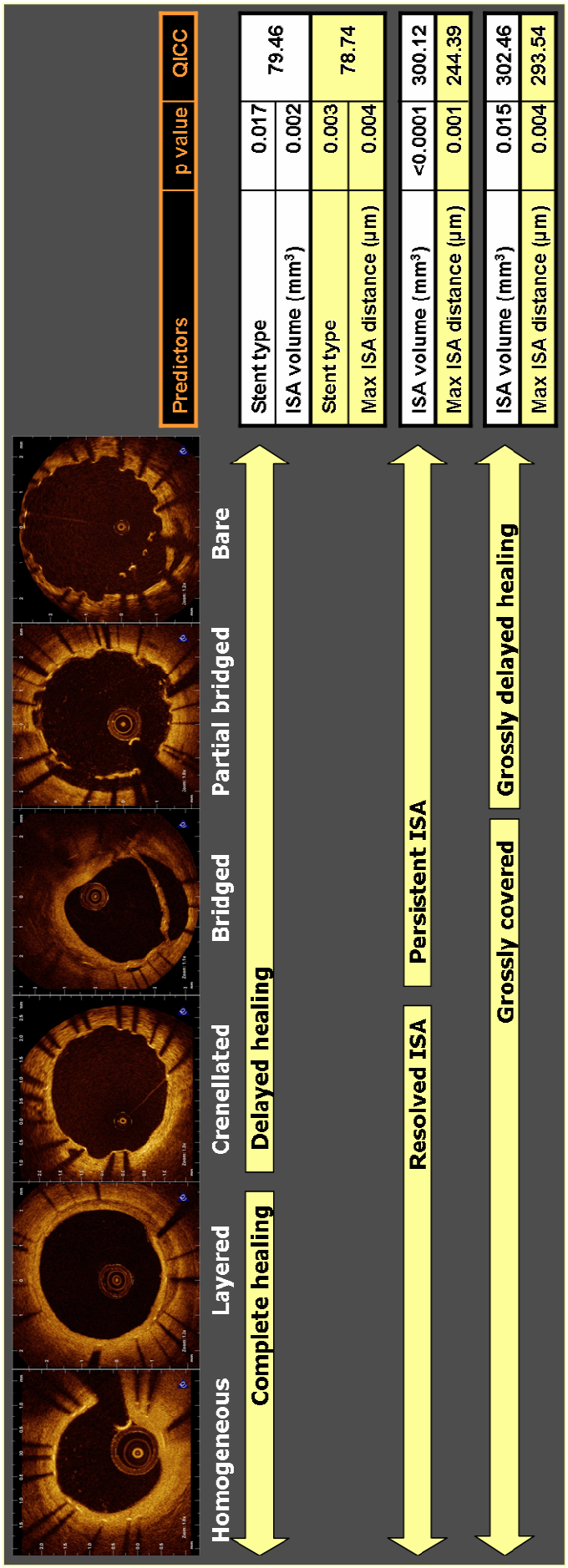

Figures legends.

Supplemental figure 1: ISA volume immediately after stent implantation (T0) and at follow-up (T1), stratified by type of stent (left panel) and by clinical indication (right panel).

AMI: Acute myocardial infarction; DCB-BMS: Drug-coated balloon in combination with BMS; EES: Everolimus-eluting stent; ISA: Incomplete stent apposition struts; SE-BMS: Self-expandable bare-metal stent; TCFA: Thin cap fibroatheroma; UA: Unstable angina; ZES: Zotarolimus-eluting stent.

Supplemental figure 2: Forest plot showing the pooled relative risk of delayed coverage at 6-13 months in malapposed vs. well-apposed segments, stratified by type of stent.
Lines represent the 95% confidence interval for the relative risk in each stent, with the pooled relative risk at the bottom.

DCB-BMS: Drug-coated balloon in combination with bare metal stent; EES: Everolimus-eluting stent; ISA: Incomplete stent apposition struts; SE-BMS: Self-expandable bare metal stent; ZES: Zotarolimus-eluting stent.

Supplemental figure 3: Predictors of complete vs. delayed healing, resolved vs. persistent ISA and grossly covered vs. grossly delayed healing patterns. Stent type and ISA size at baseline were both predictors of delayed healing, with similar predictive value of the model using either ISA volume (white cells) or maximal ISA distance per strut (yellow cells). ISA size at baseline was the only independent predictor of persistent ISA or grossly delayed coverage.

QICC: Corrected quasi-likelihood under independence model criterion.

Circulation
Cardiovascular Interventions

Vascular Tissue Reaction to Acute Malapposition in Human Coronary Arteries: Sequential Assessment With Optical Coherence Tomography

Juan Luis Gutiérrez-Chico, Joanna Wykrzykowska, Eveline Nüesch, Robert Jan van Geuns, Karel T. Koch, Jacques J. Koolen, Carlo di Mario, Stephan Windecker, Gerrit-Anne van Es, Pierre Gobbens, Peter Jüni, Evelyn Regar and Patrick W. Serruys

Circ Cardiovasc Interv. 2012;5:20-29; originally published online February 7, 2012;
doi: 10.1161/CIRCINTERVENTIONS.111.965301
Circulation: Cardiovascular Interventions is published by the American Heart Association, 7272 Greenville Avenue, Dallas, TX 75231

Print ISSN: 1941-7640. Online ISSN: 1941-7632